Solid State Science and Technology, Vol. 34, No. 1 (2026) 31-39
https://doi.org/10.66514/ssst34-1-31-39

Effect of Nanosized FeF_2 Addition on Phase Formation, Microstructure and Critical Temperature of $Tl_2Ba_2CaCu_2O_8$ Superconductor

Y.S. Ng[1], D.E. Uskenbaev[2,], Tursyntay Serua[3], Maxim Kulakov[2], Y. Khuanbay[2]*
W. Kong[1], M. N. Mohd Nasir[1], A.P.B. Ilhamsyah[1,]*

[1]Department of Applied Physics, Universiti Kebangsaan Malaysia 43600 Bangi, Selangor, Malaysia
[2]Institute of Energy, S. Seifullin Kazakh Agrotechnical Research University, Astana Kazakhstan
[3]Kazakh-British Technical University, Almaty, Kazakhstan

**Corresponding authors.(E-mail addresses: D.E. Uskenbaev: usdan@mail.ru,*
A.P.B. Ilhamsyah: ilhamsyahputraabubakar@gmail.com)

(Received: 15 June 2026 / Revised:20 July 2026 / Accepted: 1 August 2026 / Published online: 3 August 2026)

ABSTRACT

The $Tl_2Ba_2CaCu_2O_8$ (Tl-2212) phase superconductor with critical temperature 110 K, offers a better phase stability, easier synthesis control and more reproducible superconducting properties than $Tl_2Ba_2Ca_2Cu_3O_{10}$ (Tl-2223) with critical temperature 125 K, making it more suitable for systematic studies despite its slightly lower critical temperature. To enhance the critical current density, magnetic nanoparticles with size, l between the coherence length, ξ and the penetration depth, λ can be added to the Tl-2212 phase, where the particles act as effective flux pinning centers. In this study, 120 nm antiferromagnetic FeF_2 nanoparticles were added into $Tl_2Ba_2Ca_2Cu_2O_8(FeF_2)_x$ with $x = 0$ to 0.04 wt.%. The main aim was to investigate the effects of nanosized FeF_2 on the Tl-2212 phase formation and critical temperature. X-ray diffraction (XRD) analysis confirmed that a single Tl-2212 superconducting phase was formed in all FeF_2 added samples. The non-added sample exhibited a superconducting onset critical temperature ($T_{c\text{-onset}}$) of 108 K, whereas samples with FeF_2 additions of $x \leq 0.03$ wt. % retained a relatively high $T_{c\text{-onset}}$ of approximately 100 K, indicating that low FeF_2 concentrations have only a minimal effect on the onset of superconductivity. These results demonstrate that FeF_2 can be incorporated into Tl-2212 without causing significant disruption to phase formation or the critical temperature provided that the doping level is $x \leq 0.03$ wt.%. This suggests that careful FeF_2 doping could be a viable addition for optimizing microstructural and textural properties while maintaining high critical temperature.

Keywords: Tl-2212 phase; microstructure; critical temperature; X-ray diffraction

INTRODUCTION

The $Tl_2Ba_2Ca_2Cu_3O_{10}$ (Tl-2223) phase possesses a higher superconducting critical temperature, T_c (125 K) than $Tl_2Ba_2CaCu_2O_8$ (Tl-2212) with T_c = 110 K [1,2]. However, the Tl-2212 phase offers several important advantages from both experimental and practical viewpoints. Tl-2212 phase can be synthesized more easily and reproducibly, with a wider processing window and better control of phase purity, whereas Tl-2223 is highly sensitive to processing conditions and thallium loss, often leading to multiphase samples. Compared to Tl-2223 phase which has a three CuO_2-layers, the Tl-2212 has a simpler two CuO_2-layer structure and it exhibits fewer structural defects, better grain connectivity and lower anisotropy. These features result in a more stable and reproducible superconducting and transport properties, particularly in bulk and polycrystalline samples. Consequently, Tl-2212 is often preferred for systematic studies and applications where structural stability and reproducibility are essential. Several studies to improve the properties of the Tl-2212 phase continue to be reported until recently [3,4,5,6,7].

The addition of nanosized particles is one of the ways to improve the current density of this cuprate based superconductors. In this paper, the effects of 120 nm FeF_2 on the formation of the Tl-2212 phase superconductor were investigated. FeF_2 was chosen because it is paramagnetic at room temperature but antiferromagnetic at low temperatures. Nanosized FeF_2 was chosen because its size is between the coherence length, ξ and the penetration depth, λ of Tl-2212 where FeF_2 may act an effective flux pinning center for increased transport critical current density. Magnetic nanoparticles with a characteristic size (l) satisfying the condition $\xi < l < \lambda$ can interact strongly with the flux-line lattice. This interaction enhances flux pinning, resulting in the formation of a frozen-flux superconducting state and improving the stability of magnetic flux within the superconductor [8].

FeF_2 is paramagnetic at room temperature and transitions to an antiferromagnetic state is below its Néel temperature (T_n = 78.12 K). Its intrinsic (internal) magnetic field, which arises from the magnetic ordering within the material, is reported to be 32.9 T at 0 K and 2.5 T at 77 K [9]. The melting point of FeF_2, ranging from 970 °C to 990 °C at standard atmospheric pressure, is higher than the melting point (717 °C) and vaporization point (875 °C) of Tl_2O_3. These thermal and magnetic properties indicate that FeF_2 can be incorporated into the Tl-2212 system without premature melting or degradation, while its magnetic behavior may influence the superconducting characteristics at low temperatures.

This study aimed to investigate the effect of FeF_2 addition on the phase formation and superconducting critical temperature of the Tl-2212 superconductor. The samples were characterized using X-ray diffraction (XRD) to identify phase composition, scanning electron microscopy (SEM) to examine microstructural features, and four-point probe measurements to evaluate electrical resistance as a function of temperature.

MATERIALS AND METHODS

The samples were prepared using the precursor route, where appropriate amounts of high purity (99.99%) BaO, CuO, CaO were mixed with initial formula $Ba_2CaCu_2O_z$. The powders were calcined at 890 °C for 24 h with one intermittent grinding. The precursor powders were then added with Tl_2O_3 and nanosized FeF_2 (120 nm, 99.99% purity) according to the formula $Tl_2Ba_2CaCu_2O_8(FeF_2)_x$ for x = 0, 0.01, 0.03 and 0.04 wt.%. In order to compensate for the thallium lost during heating, 10% Tl_2O_3 were added to the samples. The mixing was done in a helium filled glove bag due to the hygroscopic nature of FeF_2. The mixture was pressed into pellets with 12.5 mm diameter and 2 mm thickness. The pellets were then placed in a preheated tube furnace and heated at 905 °C for 5 min in oxygen flow and oven cooled to room temperature. The oxygen flow was continued during cooling until 200 °C.

The phase was identified using the X-ray diffraction method using a Bruker D8 Advance diffractometer with CuK_α radiation with wavelength 1.5418 Å. The scan angle was between 2θ=20° and 60°. The microstructure was determined using a Philips XL 30 scanning electron microscope.

The critical temperature was measured using the resistance versus temperature measurements. The four point probe method was used to measure the resistance with silver paste as the electrical contact between the probe and the samples. The low temperature measurements were performed using the CTI Cryogenics Closed Cycle Refrigerator Model 22. A Lake Shore temperature controller model 340 was used to control the temperature. A constant current between 1 mA to 100 mA was used in the measurements.

RESULTS AND DISCUSSION

Figure 1 shows the XRD patterns of all samples. All peaks are attributed to the Tl-2212 phase and no impurity peaks were observed. The calculated unit-cell volumes derived from the lattice parameters *a, b*, and *c* show only minor variations, ranging from 436.4 to 437.3 $Å^3$ (Table 1). This narrow spread indicates that the crystal structure remains essentially unchanged across the samples, reflecting good phase stability and structural homogeneity. The small increase in unit-cell volume observed in the third set of parameters is mainly associated with a slight elongation along the *c*-axis, while the in-plane lattice constants *a* and *b* remain nearly constant. This suggests limited incorporation of Fe/F-related species into the lattice or subtle changes in interlayer spacing. At x = 0.04, both *c* and *V* decrease, implying the onset of structural instability or secondary phase formation at higher FeF_2 content. Such behavior suggests that any compositional modification or processing variation predominantly affects the interlayer spacing rather than the CuO_2 planes.

The effects of FeF_2 addition in $Tl_2Ba_2CaCu_2O_8$ can be interpreted in light of high-pressure studies, which show that superconductivity is highly sensitive to lattice distortion rather than structural phase transitions [10]. Under moderate pressure, T_c increases due to enhanced electronic coupling, but excessive compression induces distortion that suppresses superconductivity. Similarly, low FeF_2 content produces only slight lattice changes, suggesting limited incorporation or subtle interlayer modification. However, at x = 0.04, the changes in both the *c*-axis parameter and unit-cell volume indicates emerging structural instability or secondary phase formation, implying that excessive FeF_2 induces distortion analogous to high-pressure suppression of T_c. Overall, the limited fluctuation in the unit-cell volume implies minimal lattice distortion, supporting the formation of a stable Tl-2212 phase with consistent crystallographic characteristics.

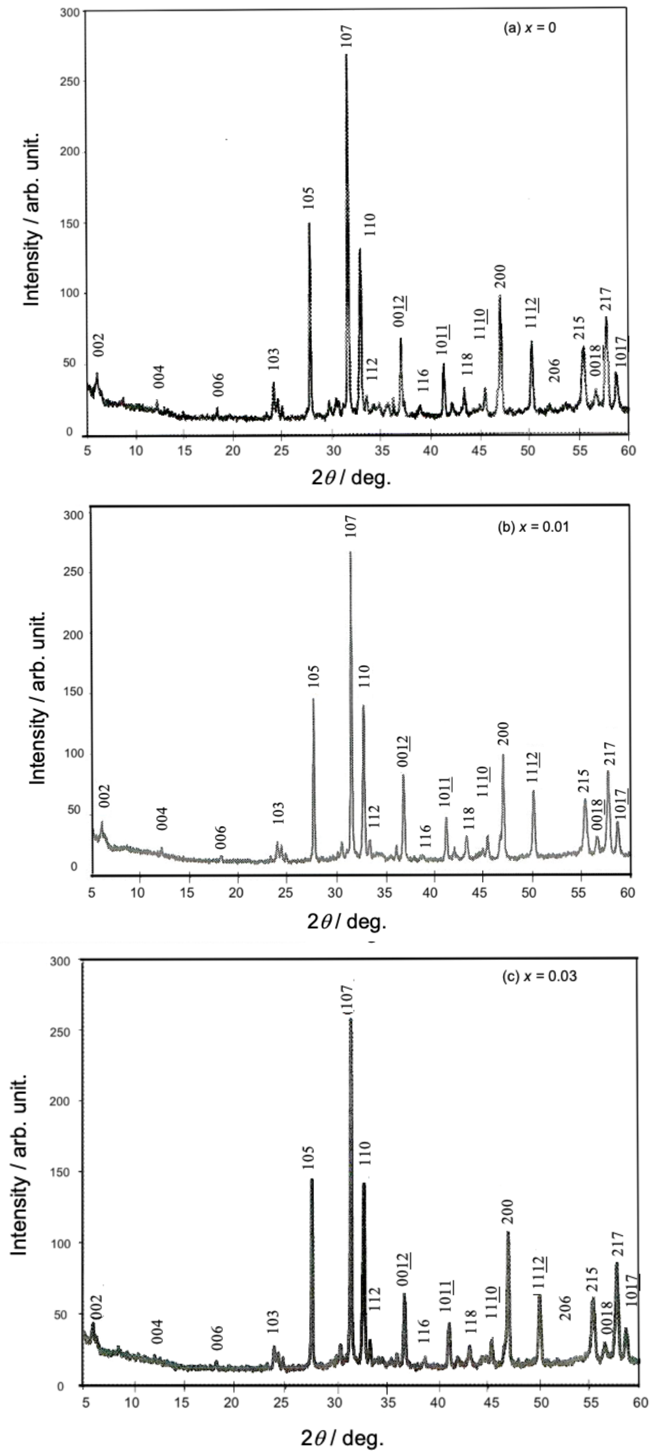

Figure 1. XRD patterns of $Tl_2Ba_2CaCu_2O_8(FeF_2)_x$ for x = 0, 0.01, 0.03 and 0.04 wt.%. All peaks are attributed to the Tl-2212 phase and no impurity peaks were observed

Figure 2 shows the SEM micrographs of the x = 0 and 0.03 samples. Contrary to the typical trend, a minimal FeF_2 addition (x = 0.03) in Tl-2212 appears to promote grain growth compared to the pure sample ($x = 0$). The pure compound shows smaller, more granular grains approximately 1–2 μm in size. In contrast, the $x = 0.03$ sample exhibits longer, well-developed plate-like grains, estimated at 3–4 μm in length. This suggests that a low FeF_2 concentration may act as a flux or sintering aid, improving crystal growth and texturing throughout the processing. Such microstructural improvement could positively influence superconducting properties by enhancing grain connectivity and alignment, highlighting a non-monotonic doping effect where a small additive optimizes morphology before larger amounts inhibit growth.

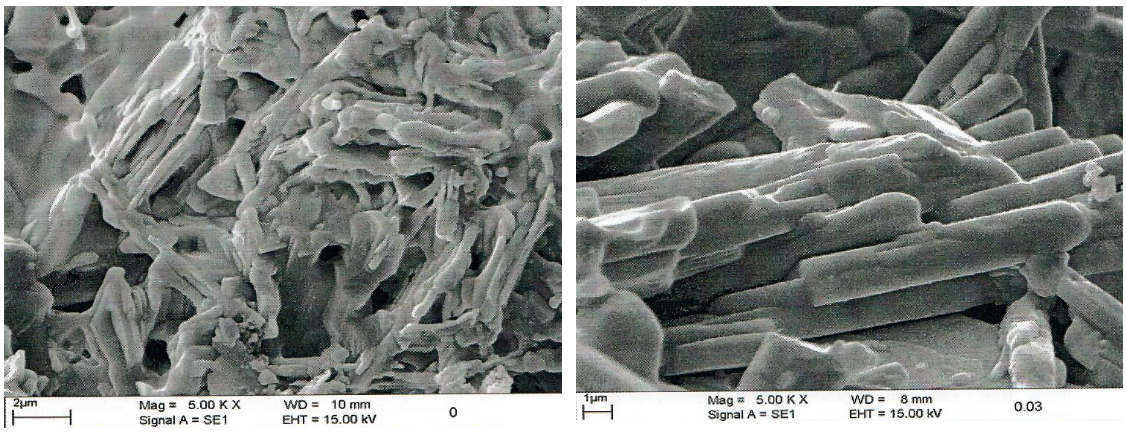

(a) (b)

Figure 2. Microstructure of $Tl_2Ba_2CaCu_2O_8(FeF_2)_x$ for (a) $x = 0$ and (b) $x = 0.03$ wt.%. with addition of FeF_2 the microstructure formed longer plate-like structure

Table 1. Lattice parameters, unit cell volume, $T_{c\text{-onset}}$, $T_{c\text{-zero}}$, T_c^{P1}, T_c^{P} and resistivity (at 300 K) for all samples

x	a / Å	b / Å	c / Å	V / Å^3	$T_{c\text{-onset}}$ /K	$T_{c\text{-zero}}$ /K	T_c^{P1}/K	T_c^{P}/K	ρ_{300K} /mΩ cm
0	3.865	3.860	29.25	436.4	108	93	107	97	16.26
0.01	3.864	3.862	29.27	436.8	100	81	93	83	5.78
0.03	3.865	3.861	29.30	437.3	100	75	98	90	7.94
0.04	3.863	3.862	29.23	436.1	77	69	75	75	8.02

Figure 3 shows the resistance versus temperature of the samples. The $T_{c\text{-onset}}$ decreases from 108 K ($x = 0$) to 100 K for $x = 0.01$–0.03, and drops sharply to 77 K at $x = 0.04$. A more pronounced suppression is observed in $T_{c\text{-zero}}$, which falls from 93 K ($x = 0$) to 81 K ($x = 0.01$), 75 K ($x = 0.03$), and 69 K ($x = 0.04$). This widening of the transition width (Figure 4) suggests increased disorder, increased superconducting inhomogeneity and enhanced scattering due to Fe incorporation. A similar behavior was observed in FeF_2-added $YBa_2Cu_3O_7$, where the superconducting transition temperature decreased abruptly for FeF_2 concentrations exceeding 0.03 wt.% [11]. This similarity suggests that the same underlying mechanism, most likely associated with enhanced magnetic scattering, increased structural disorder, or weakened superconducting coupling, is also responsible for the suppression of the transition temperature in the FeF_2-added Tl-2212 samples.

The normal-state resistivity (Table 1) at 300 K decreases significantly upon light FeF_2 addition, reaching a minimum at x = 0.01 (5.78 mΩ cm), indicating improved normal-state charge transport, which may be associated with enhanced densification or reduced porosity of the sample. However, resistivity increases again at x = 0.03 and 0.04, consistent with enhanced defect scattering.

In order to understand the transport current properties further, the dR/dT versus T curves were plotted (Figure 5). The curve generally showed two peaks; the higher temperature peak (T_c^{P1}) indicates the intragrain current and the lower temperature peak (T_c^{P}) indicates the intergrain current. For x = 0, T_c^{P1} was observed near 107 K, which coincides with $T_{c\text{-onset}}$ while the lower temperature peak T_c^{P} was observed at 97 K. This indicates that the intragrain current occurred at 107 K and the intergrain current at 97 K. The x = 0.01 sample showed intragrain currents occurred at 93 K and intergrain currents at 83 K, reflecting the suppression of both intragrain and intergrain superconductivity by FeF_2 addition. The presence of two peaks demonstrated separate intragrain and intergrain superconducting transitions, suggesting the presence of weak-link behavior between grains. The x = 0.03 sample showed T_c^{P1} and T_c^{P} at 90 K and 98 K, respectively, indicating a slight improvement of the intragrain transition compared with x = 0.01 while maintaining distinct grain-boundary coupling. The separation between T_c^{P1} and T_c^{P} remained approximately 10 K for x = 0 and 0.01, decreased to 8 K for x = 0.03, and disappeared for x = 0.04. This revealed that slightly improved grain coupling, notably for x = 0.03, which is consistent with the denser and more linked microstructure observed in the SEM image (Figure 2(b)). The x = 0.04 sample showed only one peak at 75 K which indicated that the intragrain and intergrain current occurred simultaneously at the same temperature.

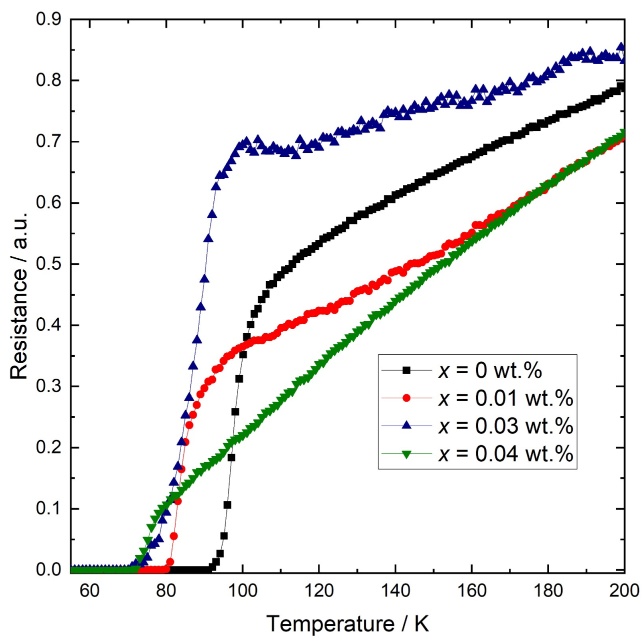

Figure 3. Electrical resistance versus temperature curves of $Tl_2Ba_2CaCu_2O_8(FeF_2)_x$ for x = 0, 0.01, 0.03 and 0.04 wt.%

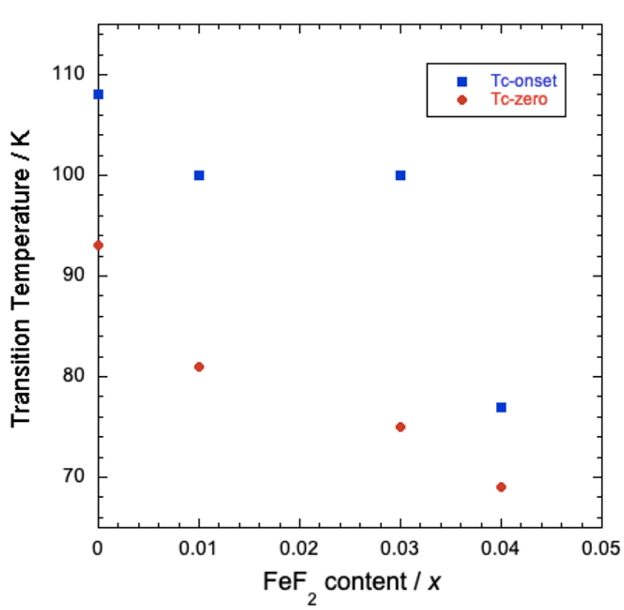

Figure 4. $T_{c\text{-onset}}$ and $T_{c\text{-zero}}$ versus FeF_2 content

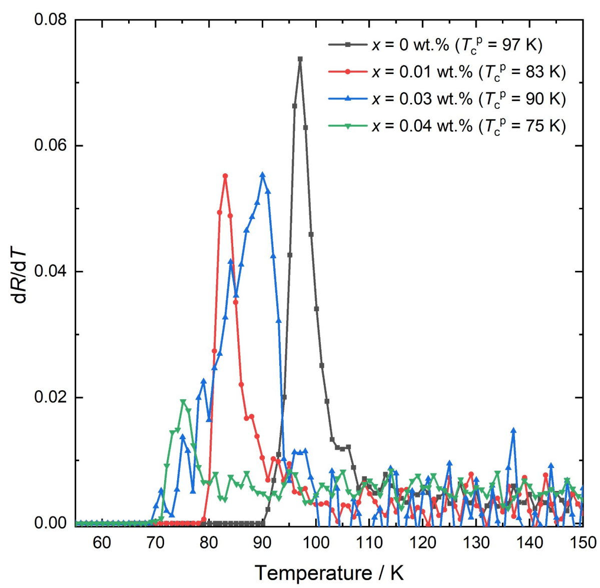

Figure 5. dR/dT versus temperature curves of $Tl_2Ba_2CaCu_2O_8(FeF_2)_x$ for $x = 0$, 0.01, 0.03 and 0.04 wt.%

These findings provide valuable insights into the role of antiferromagnetic FeF_2 nanoparticles in modifying the superconducting behavior of Tl-2212. The results may serve as a basis for further optimization of the microstructure, flux-pinning capability and intergranular connectivity, thereby improving the transport properties, particularly the critical current density. Such improvements are essential for enhancing the performance of Tl-2212 in high magnetic fields and practical operating conditions. Furthermore, the knowledge gained from this study contributes to a better understanding of the interaction between magnetic nanoparticles and high-T_c cuprate superconductors and may facilitate the development of superconducting materials with improved performance for applications in power transmission, high-field magnets, superconducting fault current limiters, magnetic energy storage systems and other advanced superconducting technologies [11,12].

CONCLUSIONS

In conclusions, the effects of antiferromagnetic nanosized FeF_2 on Tl-2212 superconductor have been investigated. Our results indicate that small FeF_2 ($x \geq 0.03$) additions kept the onset critical temperature above 100 K, while higher FeF_2 content leads to suppression of $T_{c\text{-onset}}$. The XRD diffraction patterns showed that the Tl-1212 phase was obtained for all addition levels. This indicates that this phase is stable against FeF_2 addition. Overall, the findings demonstrate that low FeF_2 additions can be introduced without significantly degrading the superconducting properties, while higher concentrations are detrimental to superconductivity and should therefore be avoided in Tl-2212 superconductors.

ACKNOWLEDGEMENTS

This research has been funded by the Science Committee of the Ministry of Science and Higher Education of the Republic of Kazakhstan (Grant No. AP26104991). The authors would like to thank the Department of Applied Physics, Universiti Kebangsaan Malaysia, for providing some of the facilities to carry out this research.

COMPETING INTERESTS

The authors declare that they have no relevant financial or non-financial interests

DATA AVAILABILITY

The datasets used and/or analyzed during the current study are available from the corresponding author upon reasonable request.

REFERENCES

[1] Parkin SSP, Lee VY, Nazzal AI, Savoy R, Beyers R. $Tl_1Ca_{n-1}Ba_2Cu_nO_{2n+3}$ (n = 1, 2, 3): A new class of crystal structures exhibiting volume superconductivity at up to ≃110 K. Physical Review Letters. 1988;61:750-753.

[2] Sheng ZZ, Hermann AM. Superconductivity in the rare-earth-free Tl-Ba-Cu-O system above liquid-nitrogen temperature. Nature. 1988;332:55-58.

[3] Subramanyam G, Ju Z, Fahmy M, Shand PM, Zhang M, Boolchand P. Processing and physical properties of single phase $Tl_2Ba_2CaCu_2O_8$ and $(Tl_{0.5}Pb_{0.5})Sr_{2-x}Ba_xCa_2Cu_3O_9$ superconductors. Applied Superconductivity 1998;4(12):591-598.

[4] Metskhvarishvili, Ioseb, Melita Menelaou, D. L. Surmanidze, Tata Lobzhanidze, A. D. Tchankvetadze, B. G. Bendeliani, G. N. Dgebuadze, V. M. Gabunia, M. R. Metskhvarishvili, and D. A. Jishiashvili. Influence of As_2O_3 vapor pressure on phase

formation and superconducting properties of Tl-2212 HTS. Low Temperature Physics 2026;52(1):85-89.

[5] Ji, Lu, Xuelian Liang, Kaiyong He, Jian Xing, Ting Xue, Tengda Xu, Litian Wang, Shengfang Zhang, Xin Zhang, Ze He, Ming He, Cheng Zeng, Shaolin Yan, and Min Feng. Growth and property analysis of large-area epitaxial Tl-2212 high-temperature superconducting films. Ceramics International 2019;45(18):24635-24641.

[6] Xu, Juan, Mingyang Qin, Jihuang Chen, Jinsong Zhang, Qiuyan Shi, Xingyu Jiang, Fucong Chen, Zhanyi Zhao, Li Xu, Jie Yuan, Beiyi Zhu, Rui Xiong, Jing Shi, Yangmu Li, Lu Ji, Qihong Chen, Kui Jin. Evolution of transport properties in $Tl_2Ba_2CaCu_2O_{8+\delta}$ films with ionic-liquid gating. Physical Reviwe Materials 2025;9:024802.

[7] Lee, Woo-Jung, Tae-Ha Hwang, Dae-Hyung Cho, Kwangsik Jeong, Soyoung Lim, Rina Kim, and Yong-Duck Chung. Effect of the post-annealing temperature on the interfacial reaction between a high-T_c superconductor and topological insulator. Advances in Electronic Materials 2024;10:2300870.

[8] Lyuksyutov IF, Naugle DG. Frozen flux superconductors. Modern Physics Letters B. 1999;13:491-497.

[9] Wertheim GK, Buchanan DNE. Temperature dependence of the Fe^{57} hyperfine splitting in FeF_2 below the Néel temperature. Physical Review 1967;161:478-482.

[10] Zhang, Jian-Bo, Viktor V. Struzhkin, Wenge Yang, Ho-Kwang Mao, Hai-Qing Lin, Yong-Chang Ma, Nan-Lin Wang, and Xiao-Jia Chen. Effects of pressure and distortion on superconductivity in $Tl_2Ba_2CaCu_2O_{8+\delta}$. Journal of Physics: Condensed Matter. 2015;27(44):445701.

[11] Abd-Shukor R, Kong I, Lim EL, Mizan NA, Alwi HA, Jumali MH, Kong W. Enhanced critical current density of FeF_2-added $YBa_2Cu_3O_7$. J Supercond Nov Magn. 2012;25(4):957-960. doi:10.1007/s10948-011-1402-3.

[12] Saifa MA, Ahmadipour M, Satgunam M, Ansari MNM, Pramono A, Siregar RR. An engineering perspective on the progress and implementation of superconducting materials: Insights from low- and high-temperature superconductors and application. Jurnal Kejuruteraan. 2025;37(7):3445-3469. doi:10.17576/jkukm-2025-37(7)-25.

[13] Arebat RAM, Awang Kechik MM, Chen SK, Lim KP, Peh HK, Shaari AH. Superconducting transition in YBCO bulk ceramics: Correlating sintering temperature, phase formation, and AC susceptibility. Sains Malaysiana. 2025;54(5):1427-1437. doi:10.17576/jsm-2025-5405-18.